Electrostatic self-assembly of macroscopic crystals using contact electrification

BARTOSZ A. GRZYBOWSKI*, ADAM WINKLEMAN, JASON A. WILES, YISROEL BRUMER AND GEORGE M. WHITESIDES*

Department of Chemistry and Chemical Biology, Harvard University, 12 Oxford Street, Cambridge, Massachusetts 02138, USA

*e-mail: bgrzybowski@gmwgroup.harvard.edu; gwhitesides@gmwgroup.harvard.edu

Published online: 23 March 2003; doi:10.1038/nmat860

Self-assembly[1–4] of components larger than molecules into ordered arrays is an efficient way of preparing microstructured materials with interesting mechanical[5,6] and optical[7,8] properties. Although crystallization of identical particles[9,10] or particles of different sizes[11] or shapes[12] can be readily achieved, the repertoire of methods to assemble binary lattices of particles of the same sizes but with different properties is very limited[13,14]. This paper describes electrostatic self-assembly[15–17] of two types of macroscopic components of identical dimensions using interactions that are generated by contact electrification[18–20]. The systems we have examined comprise two kinds of objects (usually spheres) made of different polymeric materials that charge with opposite electrical polarities when agitated on flat, metallic surfaces. The interplay of repulsive interactions between like-charged objects and attractive interactions between unlike-charged ones results in the self-assembly of these objects into highly ordered, closed arrays. Remarkably, some of the assemblies that form are not electroneutral—that is, they possess a net charge. We suggest that the stability of these unusual structures can be explained by accounting for the interactions between electric dipoles that the particles in the aggregates induce in their neighbours.

Figure 1a outlines a representative experimental protocol. Two kinds of spheres (number, N = 10–300), made of poly(methyl methacrylate) (PMMA), Teflon, polypropylene (PP) or Nylon-6,6 (1.59 mm or 3.18 mm in diameter) were placed in a square-shaped polystyrene dish whose walls had been coated with a ~300-nm film of gold. The container was connected to a linear magnetic motor, and was made to vibrate horizontally at frequencies $\omega \sim 3$–12 Hz and amplitudes $A \sim 8$–20 mm. The sidewalls of the container formed an angle $q \sim 10$–20° with the direction of motion; this orientation efficiently randomized the trajectories of the spheres colliding with the walls of the container, and allowed the spheres to visit all regions of the gold surface.

When the container vibrated, the spheres rolled over its gold-coated surface. As the spheres rolled, they separated charge triboelectrically, both with the surface of the container and with spheres made of a different material. The magnitudes and polarities of the developed charges depended on the types of the spheres used. When spheres of both types were charged with the same polarity (for example, PMMA and Nylon-6,6), they repelled all their neighbours and formed disordered, open aggregates. When spheres of one type developed a charge opposite to that of the other type, they crystallized into regular, closed arrays.

Figure 1b shows a square lattice formed by self-assembly of equal numbers of PMMA and Teflon spheres. The spheres were initially randomly distributed over the surface, and were first gently agitated ($\omega \sim 3$ Hz, $A \sim 20$ mm) for one minute, and then shaken vigorously ($\omega \sim 8$ Hz, $A \sim 8$ mm) for approximately five minutes. During the period of gentle shaking, the spheres formed small clusters that subsequently—under vigorous agitation—aggregated into an extended lattice. When the assembly was attempted without the period of gentle shaking, the spheres charged rapidly (before forming clusters), and their collisions were too vigorous to allow 'nucleation' of clusters and formation of an ordered lattice. On the other hand, when the agitation was gentle at all times, the clusters did form, but they never assembled into larger structures.

Measurements using a Faraday cup confirmed that the PMMA spheres charged positively, and the Teflon spheres negatively (Fig. 1c). Throughout the experiment, the ratio of charges on the two kinds of spheres remained close to –1 (average along charging curve $\langle Q_{\mathrm{Tef}}(t)/Q_{\mathrm{PMMA}}(t)\rangle \sim -1.25$, where t is time). To visualize the distribution of charge developed on the surfaces of the spheres, we dusted them with fine (1–2 μm) graphite powder. We found no systematic variations in the amount of graphite adsorbed on different portions of the spheres (for example, portions closest to the surface of the container, and those furthest from it), indicating that charge was distributed uniformly over their surfaces. We also found that self-assembly was to a good approximation insensitive to the variations in ambient humidity (for 8% < RH < 50%) and to electrical bias (up to ±10 kV with respect to a disc counter electrode placed ~10 cm above the container) applied to the gold surface, and that the morphology of the final structure was independent of whether all the beads were placed in the container before agitation started, or whether some spheres were added to an already-assembled structure.

Self-assembly of different numbers of spheres of each type gave different types of lattices. Figure 2 shows the square, pentagonal and hexagonal arrays that formed from different numbers of Nylon-6,6 (N_{Nyl}) and Teflon (N_{Tef}) spheres. We used Nylon-6,6 instead of PMMA because the magnitudes of charge developed on the Nylon-6,6 spheres were almost equal to those on the Teflon beads (time average along

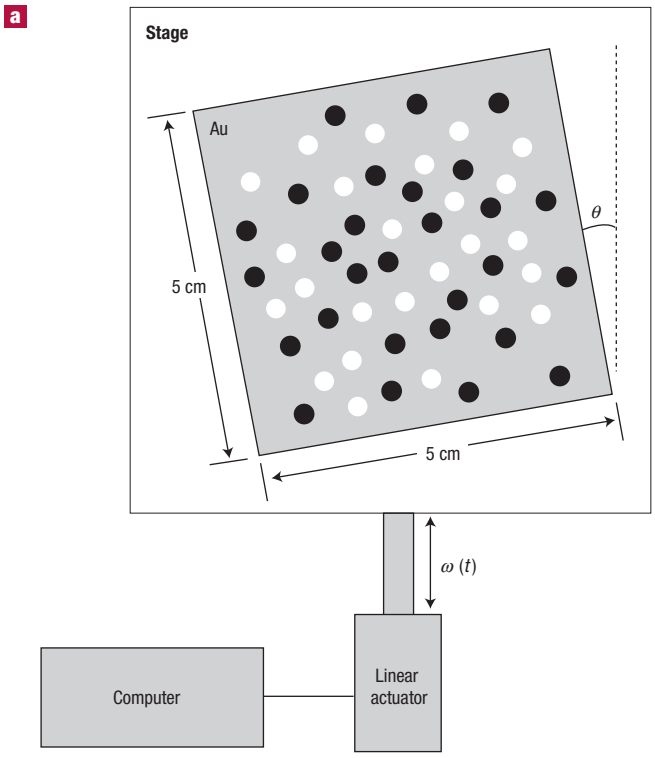

Figure 1 Electrostatic self-assembly (ESA) of polymeric spheres. a, Experimental arrangement for ESA (viewed from above). Uncharged dielectric objects—here, spheres—of two types are placed in a polystyrene container of dimensions length ~5 cm × width ~5 cm × height ~2 cm, and having its walls covered with gold. When the container is made to vibrate horizontally with frequency $\omega \sim$ 3–12 Hz and amplitude of vibration $A \sim$ 8–20 mm, the spheres organize into an ordered lattice. **b**, Photograph of a square lattice formed from equal numbers of Teflon (white) and PMMA (clear) spheres 1.59 mm in diameter. **c**, At all times during the assembly, the charges on Teflon and PMMA spheres were of similar magnitudes but opposite polarities. The initial rates of charging were approximately +0.016 nC s^{-1} for PMMA spheres and –0.019 nC s^{-1} for Teflon. Approximately 30 seconds after the start of agitation, the charges reached their steady-state, maximal values of $Q_{PMMA}(max) \sim +0.31$ nC and $Q_{Tef}(max) \sim -0.38$ nC. Every entry in the plot represents an independent experiment in which 60 spheres each of PMMA and Teflon were caused to vibrate ($\omega = 3$ Hz, $A = 20$ mm) under ambient conditions (~24% RH) for a specified time. Each value is the average of the charge measured on 25–35 individual spheres using a Faraday cup connected to a digital electrometer. The error bars represent the standard deviation for each set of measurements.

charging curve $\langle Q_{Nyl}(t)/Q_{Tef}(t)\rangle \sim -0.98$); this equality simplified subsequent theoretical analysis.

When the ratio, N_{Nyl}/N_{Tef}, of the numbers of spheres of different types was close to unity, square lattices formed. When one type of sphere was present in excess, the spheres arranged themselves into either local pentagonal aggregates or extended hexagonal lattices. For $N_{Nyl}/N_{Tef} < 1$, the Nylon-6,6 spheres organized themselves into an open hexagonal array, and the space between them was occupied by Teflon spheres—five (pentagonal aggregates) or six (hexagonal lattice) around each Nylon-6,6 sphere. Conversely, when $N_{Nyl}/N_{Tef} > 1$, it was the Teflon spheres that arranged into an open, hexagonal array with each Teflon sphere surrounded by five or six Nylon-6,6 spheres. As in the case of the PMMA/Teflon system, self-assembly was insensitive to ambient conditions, electrical bias applied to the gold surface, and the order in which beads were added. These observations suggested that the lattices were steady-state products of self-assembly, and that for a given number of spheres, the course of electrostatic self-assembly (ESA) depended only on the nature of electrostatic interactions between them.

To verify this hypothesis, we used Simulated Annealing[21] and Parallel Tempering Monte Carlo[22] (PTMC; see Supplementary Information for details) algorithms to model the self-assembly of charged spheres. On the basis of the experimental results, the charges on the spheres of different types were assigned equal magnitudes and opposite signs. Each sphere was represented as a point charge located at the centre of the sphere. The point charges interacted with one another coulombically with the energy

$$U_{ij}^{CH-CH} = Q_i Q_j / r_{ij}$$

where r_{ij} is the distance between the centres of spheres i and j. Simulations accounting only for pairwise charge–charge interactions failed to reproduce formation of patterns other than square, and predicted pentagonal and hexagonal arrays to be unstable.

It was possible to simulate the formation of electrically non-neutral pentagonal and hexagonal assemblies by including the effects of electrical polarization. Consider two oppositely charged ($Q_1 = -Q_2$) dielectric spheres **1** and **2** of equal radii a. The electrical field produced by sphere **1** induces an electric dipole in sphere **2**. This dipole is oriented in the direction of the field produced by **1**, and its magnitude is approximately[23]

$$p_{12} = \left(\frac{\varepsilon_2 - 1}{\varepsilon_2 + 2}\right) a^3 E_{12}$$

where $E_{12} = Q_1/r_{12}^2$ is the electric field produced by **1** evaluated at the centre of **2**, and ε_2 is the dielectric constant of the material from which

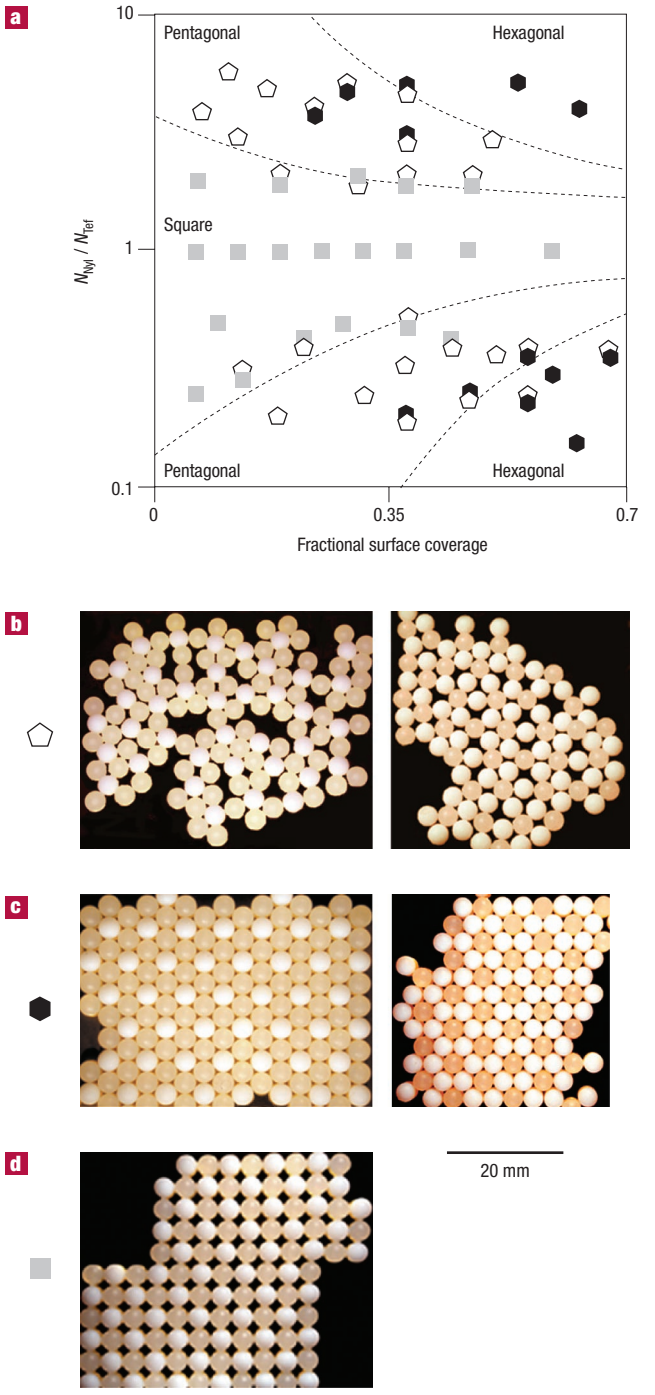

Figure 2 ESA of different numbers of Teflon and Nylon-6,6 spheres. a, Phase diagram indicating the geometries of the lattices assembled for different total (horizontal axis) and relative (vertical axis) numbers of Teflon and Nylon-6,6 spheres. The fractional surface coverage (FSC) is defined as the ratio of the sum of cross-sectional areas of the spheres to the area of the container (25 cm^2). Square lattices (indicated by grey squares) form when the numbers of spheres of different types are similar. Pentagonal and hexagonal arrays (indicated by open pentagons and black hexagons, respectively) assemble when beads of one type are present in excess. For some compositions, the spheres can self-assemble into one of the two possible lattices. In these cases, the geometry that is observed most often is indicated by the foreground symbol. **b**, Pentagonal arrays formed by 160 spheres (FSC ~50%). In the picture on the left, there are 120 Nylon-6,6 spheres (off-white) and 40 Teflon (white) ones; in the picture on the right, 120 Teflon and 40 Nylon-6,6 spheres. **c**, Hexagonal lattices formed by 190 spheres (FSC ~60%): 145 Nylon-6,6 and 45 Teflon (left picture) and 130 Nylon-6,6 and 60 Teflon (right picture). **d**, Square array self-assembled from 60 Nylon-6,6 and 60 Teflon spheres. In **b** and **c**, the excess spheres expelled towards the edges of the container are not shown. In all cases, the assemblies were generated by vibrating the container horizontally at frequency $\omega = 3$ Hz and amplitude $A = 20$ mm for 1 min and then at $\omega = 8$ Hz and $A = 8$ mm for 3–5 min.

sphere 2 is made. The energy of the charge-induced dipole interaction between the spheres is then given by

$$U_{1,2}^{CH-D} = -\vec{p}_{12}\cdot\vec{E}_{12} - \vec{p}_{21}\cdot\vec{E}_{21} = -\left(\frac{\varepsilon_1 - 1}{\varepsilon_1 + 2} + \frac{\varepsilon_2 - 1}{\varepsilon_2 + 2}\right) a^3 Q_1^2 / r_{12}^4$$

in which the $\vec{p}_{ij}\cdot\vec{E}_{ij}$ term accounts for the interaction of the dipole induced in j with the field produced by i. If the charges on the two spheres have opposite signs, the charge-induced dipole interaction lowers the interaction energy (that is, makes it more favourable) by $U_{1,2}^{CH-D}$; for two touching spheres (3.18 mm in diameter; $\varepsilon \sim 3$), this energetic gain is approximately 10% of the total energy of interaction. A similar derivation for the case of two like-charged spheres shows that charge-induced dipole interaction reduces the total, repulsive interaction energy by $U_{1,2}^{CH-D}$. The overall effect is that the attractive interactions between the oppositely charged spheres are strengthened, while the repulsive ones between like-charged spheres are weakened.

With polarization effects included, and approximating the total energy of an ensemble as a sum of pair-wise interactions between the spheres, PTMC simulations predicted the hexagonal and pentagonal arrays to be stable. For all compositions, the energies of these phases were significantly lower than those of random configurations of spheres. In some cases, however, our model predicted square arrays slightly lower in energy (by less than one percent) than experimentally observed pentagonal or hexagonal ones. In these instances, the inability to discriminate between energetically similar polymorphs reflects the limitations of our model, which assumes independence of multiple dipoles induced on each sphere by its neighbours.

When the materials from which the spheres were made charged at different rates, structures of different morphologies could form during the course of charging. Figure 3 illustrates the assembly of 40 Teflon and 80 PP spheres agitated at $\omega \sim 9$ Hz and $A \sim 10$ mm. The Teflon spheres charged more rapidly than the PP ones (Fig. 3a). When, after approximately 30 seconds from the start of agitation, the ratio of charges Q_{Tef}/Q_{PP} was close to –2, the spheres organized into a hexagonal structure (Fig. 3b, left). PTMC simulations predicted this structure to be a global energy minimum of the system. As the agitation continued, the magnitudes of charges on the Teflon and PP spheres equalized. The hexagonal arrangement became energetically unstable. After ~15 minutes, approximately half of the PP spheres were expelled towards the walls of the container, and the morphology of the aggregate changed to square (Fig. 3b, right). Simulations found this square lattice to be the minimal energy structure for $Q_{Tef}/Q_{PP} \sim -1$. We note that for the switching between the lattices to occur, the kinetics of charging must be commensurate with the kinetics of structure formation, and the kinetic energies of the spheres must be large enough to overcome the packing in an energetically unfavourable lattice. For example, if the spheres are fully charged before the lattices nucleate (Fig. 3c, $\omega \sim 11$ Hz and $A \sim 11$ mm), they never crystallize in a hexagonal array, but rather go immediately into a square one. On the other hand, if the spheres charge slowly, and their kinetic energies are small (Fig. 3c, $\omega \sim 8$ Hz and $A \sim 8$ mm), the system evolves into a hexagonal pattern, and cannot switch into a square lattice even when the magnitudes of charges on the spheres of different types equalize.

ESA is not limited to components of spherical geometries. Figure 4 shows spheres, a checkerboard array, and a rod-like structure of

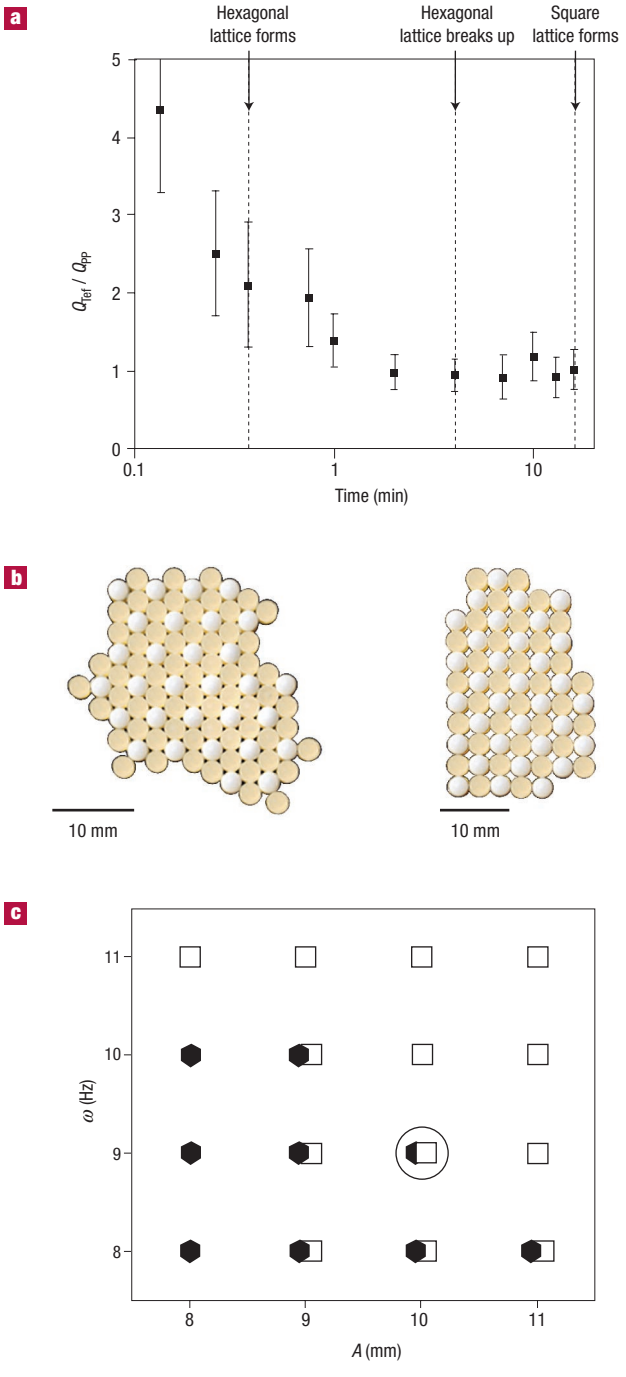

Figure 3 **Pattern switching in an ensemble of 40 Teflon and 80 PP spheres agitated at ω = 9 Hz and A = 10 mm. a**, The plot shows the ratio of magnitudes of charges on the spheres of different types as a function of time. Each point corresponds to an independent experiment starting from a random configuration of spheres. The ratio of charges in each experiment was calculated from the average charge per sphere for Teflon and for PP. The error bars correspond to the standard deviation of the ratio of charges. **b**, When $Q_{Tef}/Q_{PP} \sim -2$, the spheres form a hexagonal lattice (left) that subsequently changes to a square one ($Q_{Tef}/Q_{PP} \sim -1$, right). **c**, Phase diagram indicating the morphologies of patterns observed for different values of the frequency and amplitude of agitation: open squares: square lattice; black hexagons: hexagonal lattice; black hexagons over open squares: hexagonal lattice in which isolated domains switch to square packing (partial switching); open square over black hexagon (circled data point for which assembly pictures and kinetics were measured): hexagonal lattice switching to square lattice (complete switching).

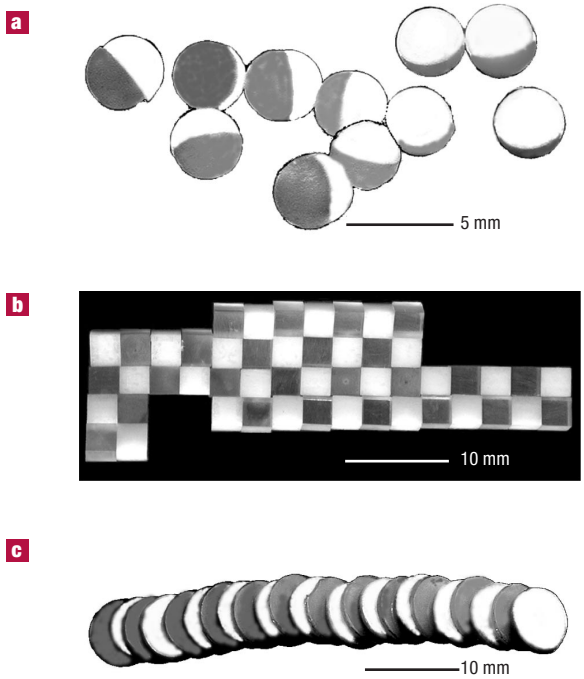

Figure 4 **ESA of non-spherical, millimetre-sized objects assembled in a rotating glass cylinder of diameter ~4 cm. a**, Photograph of spheres (diameter = 3.18 mm) formed by heterodimerization of Teflon (white) and Nylon-6,6 (grey) hemispheres. The assembled spheres interacted weakly with one another, and a higher order structure was not formed. Approximately 60% of the hemispheres heterodimerized into spheres; those that did not assemble are not shown. **b**, Photograph of a checkerboard structure of Teflon (white) and PMMA (clear) cubes (3.18 mm). **c**, Rod-like assembly of alternating disks (diameter ~ 7.5 mm and thickness = 0.793 mm) of Teflon (white) and Nylon-6,6 (grey). In (**a**–**c**), the long axis of the rotating cylinder was initially inclined by ~25° with respect to the horizontal. The assembling objects were confined to one end of the cylinder, and exchanged charge with both its concave surface and with its flat, bottom face. As a result, the surfaces of the assembling particles charged more uniformly than in a cylinder rotating around a horizontal axis. Once the objects were fully charged (after ~3–5 min at 47% RH), the inclination was reduced to 0° (horizontal) while continuing to rotate the cylinder at $\omega \approx 2$ Hz. The disordered collection of charged objects elongated along the length of the tube and assembled into ordered structures.

alternating materials formed from hemispheres (Teflon and Nylon-6,6), cubes and disks, respectively. Because flat surfaces of the non-spherical components tend to stick to flat supports against which they tribocharge, we caused tribocharging and self-assembly to occur in these instances inside a large glass cylinder (~4 cm in diameter) that rotated along its long axis with angular frequency ~2 Hz. When the cylinder rotated, the flat faces of the self-assembling particles could come into intimate contact with each other, but not with the curved support.

Self-assembly based on contact electrification appears to be a versatile method of assembling macroscopic dielectric particles of various shapes into extended structures.

Because electrostatic forces scale with surface area, whereas gravitational forces scale with volume, extensions of ESA to smaller length scales will require new methods of agitation, possibly with acoustic waves. Also, at smaller scales, the magnitudes of induced dipoles (scaling with the cube of a particle's radius) become negligible, so that the charge–charge interactions should dominate the morphologies of lattices. Under these conditions, lattices other than square could be prepared only if the components of different types

would charge to different degrees. Because, to a good approximation, contact electrification is a surface phenomenon, assemblies more complex than those described here could also be formed if different regions of assembling objects were patterned with thin films of different dielectric materials. Such patterning might endow electrostatic interactions with directionality and specificity, and could be the basis of self-assembly of three-dimensional colloidal crystals of different compositions and space groups.

Received 7 October 2002; accepted 24 February 2003; published 23 March 2003.

References

1. Philp, D. & Stoddart, J. F. Self-assembly in natural and unnatural systems. *Angew. Chem. Int. Edn Engl.* **35,** 1155–1196 (1996).
2. Whitesides, G. M. & Grzybowski, B. A. Self-assembly at all scales. *Science* **295,** 2418–2421 (2002).
3. Fendler, J. H. Chemical self-assembly for electronic applications. *Chem. Mater.* **13,** 3196–3210 (2001).
4. Grzybowski, B. A., Stone, H. A. & Whitesides, G. M. Dynamic self-assembly of magnetized, millimetre-sized objects rotating at a liquid-air interface. *Nature* **405,** 1033–1036 (2000).
5. Ito, K., Sumaru, K. & Ise, N. Elastic properties of colloidal crystals. *Phys. Rev. B* **46,** 3105–3107 (1992).
6. Schope, H. J., Decker, T. & Palberg, T. Response of the elastic properties of colloidal crystals to phase transitions and morphological changes. *J. Chem. Phys.* **109,** 10068–10074 (1998).
7. Joannopoulos, J. D., Meade, R. D. & Winn, J. N. *Photonic Crystals* (Princeton Univ. Press, Princeton, New Jersey, 1995).
8. Reese, C. E., Baltusavich, M. E., Keim, J. P. & Asher, S. A. Development of an intelligent polymerized crystalline colloidal array colorimetric reagent. *Anal. Chem.* **73,** 5038–5042 (2001).
9. Xia, Y., Gates, B., Yin, Y. D.& Lu, Y. Monodispersed colloidal spheres: Old materials with new applications. *Adv. Mater.* **12,** 693–713 (2000).
10. Van Blaaderen, A., Ruel, R. & Wiltzius, P. Template-directed colloidal crystallization. *Nature* **385,** 321–324 (1997).
11. Kiely, C. J., Fink, J., Burst, M., Bethell, D. & Schiffrin, D. J. Spontaneous ordering of bimodal ensembles of nanoscopic gold clusters. *Nature* **396,** 444–446 (1998).
12. Adams, M., Dogic, Z., Keller, S. L. & Fraden, S. Entropically driven microphase transitions in mixtures of colloidal rods and spheres. *Nature* **393,** 349–352 (1998).
13. Bowden, N., Choi, I. S., Grzybowski, B. A. & Whitesides, G. M. Mesoscale self-assembly of hexagonal plates using lateral capillary forces: synthesis using the "capillary bond". *J. Am. Chem. Soc.* **121,** 5373–5391 (1999).
14. Grzybowski, B. A., Bowden, N., Arias, F.,Yang, H. & Whitesides, G. M. Modeling of menisci and capillary forces from millimeter to the micrometer size range. *J. Phys. Chem. B* **105,** 404–412 (2001).
15. Kumar, A. *et al.* Linear superclusters of colloidal gold particles by electrostatic assembly on DNA templates. *Adv. Mater.* **13,** 341–344 (2001).
16. Tien, J., Terfort, A. & Whitesides, G. M. Microfabrication through electrostatic self-assembly. *Langmuir* **13,** 5349–5355 (1997).
17. Caruso, F., Lichtenfeld, H., Giersig, M. & Mohwald, H. Electrostatic self-assembly of silica nanoparticle - Polyelectrolyte multilayers on polystyrene latex particles. A. *J. Am. Chem. Soc.* **120,** 8523–8524 (1998).
18. Horn, R. G., Smith, D. T. & Grabbe, A. Contact electrification of a surface and relation to acid-base interactions. *Nature* **366,** 442–443 (1993).
19. Horn, R. G. & Smith, D. T. Contact electrification and adhesion between dissimilar materials. *Science* **256,** 362–364 (1992).
20. Lowell, J. & Rose-Innes, A. C. Contact electrification. *Adv. Phys.* **29,** 947–1023 (1980).
21. Kirkpatrick, S., Gelatt, C. D. & Vecchi, M. P. Optimization by simulated annealing. *Science* **220,** 671–680 (1983).
22. Neirotti, J. P., Calvo, F., Freeman, D. L. & Doll, J. D. Phase changes in a 38-atom Lennard-Jones clusters. I. A parallel tempering study in the canonical ensemble. *J. Chem. Phys.* **112,** 10340–10349 (2000).
23. Jackson, J. D. *Classical Electrodynamics* 2nd edn 135–155 (Wiley, New York, 1975).

Acknowledgements

This work was supported by the Department of Energy (award 00ER45852). J.A.W. was supported by the Natural Sciences and Engineering Research Council of Canada. A.W. was supported by the Biophysics Training Grant. Y.B. was supported by the National Science Foundation. The authors would like to thank A. Epstein (The Ohio State University) for useful discussions.

Correspondence and requests for materials should be addressed to B.A.G. or G.M.W.

Supplementary Information is available on the *Nature Materials* website (http://www.nature.com/naturematerials).

Competing financial interests

The authors declare that they have no competing financial interests.